

## Photochemical Isomerization Reactions of Cyanopyrroles: A Theoretical Study

Ming-Der Su\*

Department of Applied Chemistry, National Chiayi University, Chiayi 60004, Taiwan

Received: June 13, 2006; In Final Form: September 7, 2006

The mechanisms of the photochemical isomerization reactions were investigated theoretically using a model system of 2-cyanopyrrole and 2-cyano-5-methylpyrrole with the CASSCF (eight-electron/seven-orbital active space) and MP2–CAS methods and the 6–311(d,p) basis set. The structures of the conical intersections, which play a decisive role in such phototranspositions, were obtained. The intermediates and transition structures of the ground state were also calculated to assist in providing a qualitative explanation of the reaction pathways. Our model investigations suggest that the preferred reaction route for the cyanopyrroles is as follows: reactant  $\rightarrow$  Franck–Condon region  $\rightarrow$  conical intersection  $\rightarrow$  photoproduct. In particular, the conical intersection mechanism found in this work gives a better explanation than the previously proposed internal cyclization-isomerization mechanism and supports the experimental observations. In addition, we suggest a simple p- $\pi$  orbital topology model, which can be used as a guide tool to predict the location at which conical intersections are likely to occur, as well as the conformations of the phototransposition products of various heterocycles.

## I. Introduction

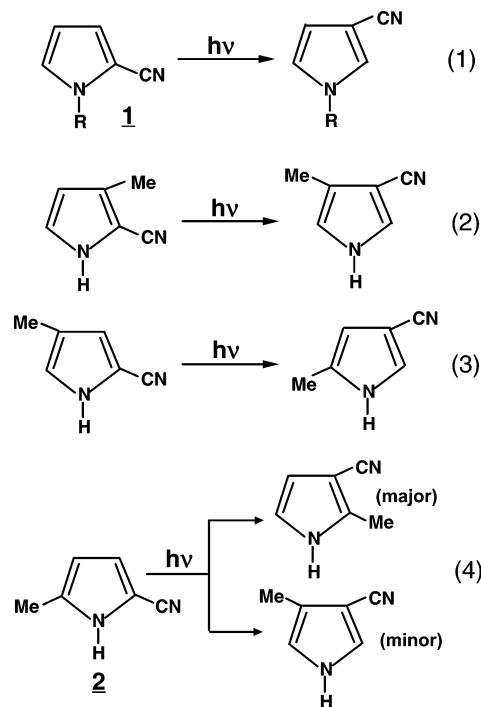
The photoisomerization chemistry of five-membered heterocycles has been the subject of extensive experimental as well as theoretical studies in the past forty years.<sup>1</sup> From the large body of experimental evidence, it was found that different product yields and byproducts are obtained dependent on the heteroatom in the ring. Most of them have been related to the isomerization reactions that result in an interchange of ring atoms.

Pyrroles, the important units in hemoglobin and chlorophyll, also undergo molecular reorganization under the influence of UV light. Hiroaka was the first to show that 2-cyanopyrrole (**1**) and its *N*-methyl analogue rearrange photochemically to the corresponding 3-cyano isomer (eq 1).<sup>2</sup> In addition, no other isomerizations take place at low temperature.<sup>3</sup> Similar results were reported for various substituted cyanopyrroles as collected in Scheme 1.<sup>3,4</sup> These reactions have been supposed to proceed via an internal cyclization-isomerization mechanism similar to those in the photochemical rearrangements of oxazole and thiophene derivatives.<sup>1,3,4</sup> Furthermore, experimental evidence also indicates that two kinds of photoproducts occur with different yields in the photoreactions of 2-cyano-5-methylpyrrole.<sup>3,4</sup> See eq 4 in Scheme 1.

It is these fascinating experimental results that aroused our interest. Theoretical investigations of pyrroles are scarce. To the best of our knowledge, only one theoretical study has reported photochemical mechanisms of cyanopyrrole.<sup>5</sup> Jug and co-workers have examined the photochemical isomerization of 2-cyanopyrrole to 3-cyanopyrrole and proposed a reaction mechanism that proceeds via bicyclic intermediates, using the semiempirical MO SINDO1 method. Hence, it is necessary to resort to more sophisticated theoretical studies to obtain a better understanding of the mechanisms of the photorearrangement reactions of pyrroles.

\* To whom correspondence should be addressed. E-mail: midesu@mail.ncyu.edu.tw.

## SCHEME 1



In the present work, we give a deeper insight into the seemingly complex mechanism of cyanopyrrole photorearrangements. A theoretical study of the photoisomerization of both 2-cyanopyrrole (**1**) and 2-cyano-5-methylpyrrole (**2**) was undertaken. These were chosen as model systems because experiments on the compounds were available for comparison. In the following sections we describe the method and present the results for the phototransposition reactions of such aromatic five-membered heterocycles in detail. Conical intersection regions<sup>6</sup> on the potential surface, where decay to the ground-state surface can occur, have been located, and ground-state reaction paths

leading from these conical intersections to a variety of products have been identified. On the basis of this information, the reaction process is explained. It will be shown below that the conical intersections<sup>6</sup> play a crucial role in the photoisomerization reactions of cyanopyrroles.

## II. Methodology

All geometries were fully optimized without imposing any symmetry constraints, although in some instances the resulting structures show various elements of symmetry. The CASSCF calculations were performed using the MCSCF program released in GAUSSIAN 03.<sup>7</sup>

The active space for describing the photorearrangements of cyanopyrroles comprises eight electrons in seven orbitals, i.e., five  $p$ - $\pi$  orbitals plus the  $\sigma(\text{C}-\text{N})$  and  $\sigma^*(\text{C}-\text{N})$  orbitals were considered to be active space, while others were considered to be inactive space. The CASSCF method was used with the 6-311G(d) basis sets for geometry optimization (vide infra). The optimization of conical intersections was achieved in the  $(f - 2)$ -dimensional intersection space using the method of Bearpark et al.<sup>8</sup> implemented in the Gaussian 03 program. Every stationary point was characterized by its harmonic frequencies computed analytically at the CASSCF level. Localization of the minima, transition states, and conical intersection minima has been performed using Cartesian coordinates; therefore, the results are independent of any specific choice of internal variables.

To correct the energetics for dynamic electron correlation, we have used the multireference Møller–Plesset algorithm<sup>9</sup> as implemented in the program package GAUSSIAN 03. The active space was chosen the same as the above CASSCF study. Unless otherwise noted, the relative energies given in the text are those determined at the MP2–CAS–(8,7)/6-311G(d) level using the CAS(8,7)/6-311G(d) (hereafter designed MP2–CAS and CASSCF, respectively) geometry.

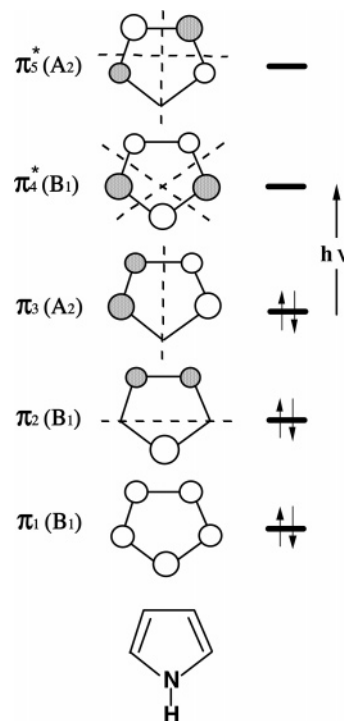
## III. General Considerations

In this section, we will analyze the electronic structures of cyanopyrrole, which forms the basis for this study. It was reported that for cyanopyrroles, experimentalists have found no indication for participation of a triplet state.<sup>2–4</sup> Triplet states therefore play no role in the reactions studied in the present work. For this reason, the photochemical transposition reactions of cyanopyrroles should proceed on singlet surfaces, and also should only involve the  $\pi \rightarrow \pi^*$  transition. We shall therefore focus on  $^1(\pi, \pi^*)$  surfaces from now on.

A general outline of the five  $p$ - $\pi$  orbitals in pyrrole has been given previously,<sup>10</sup> and is shown explicitly in Scheme 2. In the symmetry consideration we used the  $C_{2v}$  symmetry of the ring without substituents. As can be seen in Scheme 2, the lowest singlet  $\pi \rightarrow \pi^*$  excitation is the singlet  $\pi_3 \rightarrow \pi_4^*$  transition. Its irreducible representation is  $^1B_2$ . The experimental data for 2-cyanopyrrole (**1**) show that this transition has a very strong absorption band at either 4.99<sup>11</sup> or 5.04 eV.<sup>5</sup> Agreement between our calculated and the previous experimental data was good. However, the strong experimental band at 4.99 or 5.04 eV had a lower energy than the calculated one at 5.23 (CASSCF) or 5.38 eV (MP2–CAS).<sup>12</sup> We felt, however, that the accuracy of the present model calculations was sufficient for the following investigations of the mechanisms of photochemical transposition reactions.

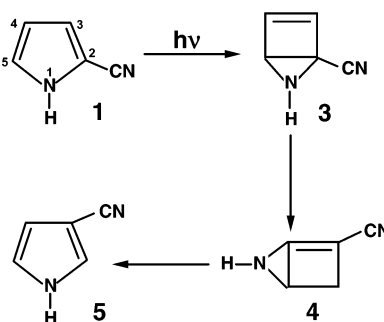
Furthermore, as already mentioned in the Introduction, the photoisomerization of cyanopyrroles appears to follow the internal cyclization-isomerization sequence, which was first

SCHEME 2

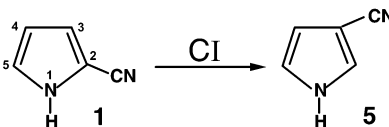


SCHEME 3

Path I:

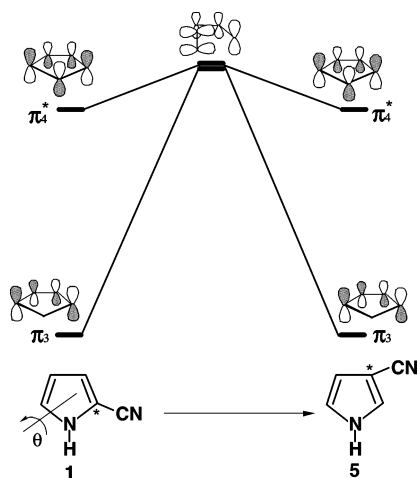


Path II:



proposed by Barltrop and co-workers.<sup>3</sup> Behrens and Jug investigated this mechanism by using the SINDO1 method.<sup>5</sup> According to their study, as shown in Scheme 3 (path I), the first reaction step is an internal cyclization which occurs via a minimum (**3**) on the excited singlet surface. From there, a radiationless transition leads to the ground-state surface. On the ground-state surface either a 1,3-sigmatropic shift of the NH group to give (**4**) or a back reaction to the reactant (**1**) takes place. The former can then react by ring opening to give 3-cyanopyrrole (**5**). Nevertheless, the energetics of the minima and transition structures that should play a role in such cyanopyrrole isomerizations were based only on the semiempirical method. Besides this, no other available mechanism was considered in their study. It is probable that a somewhat different approach, and emphasis on other aspects of the reaction, may

## SCHEME 4



open up a new perspective in the understanding and interpretation of the observed photochemical reaction behavior of pyrroles.

The next concern for the photochemical mechanism is the location of the conical intersection of excited- and ground-electronic states. Indeed, it has been shown recently that conical intersections play a decisive role in many photochemical reactions.<sup>6</sup> In principle, conical intersections correspond to crossings between states of the same multiplicity (most commonly singlet–singlet). In suitable conditions, conical intersection represents very efficient “funnels” for radiationless deactivation or chemical transformation in the system. In this work, we shall use the  $p$ - $\pi$  orbital model to search for the conical intersections of the photoisomerization reaction of the cyanopyrrole molecule which is isoelectronic with benzene. Scheme 4 shows the qualitative potential energy curves for the  $S_0$  and  $S_1$  states of pyrrole as a function of rotation about the  $N$ – $C$  chemical bond (i.e., the rotation angle  $\theta$ ). By twisting the  $N=C$   $\pi$  bond in pyrrole, both  $\pi_3$  and  $\pi_4^*$  are raised in energy due to increased antibonding interactions. Finally, at a specific geometry, these  $\pi$  orbitals become degenerate (calculated  $100^\circ$  rotation, see Figure 1<sup>13</sup>). Accordingly, this excitation removes the barrier to rotation about the former  $N$ – $C$  axis and rotation toward a nearly perpendicular orientation of the  $p$ - $\pi$  orbitals

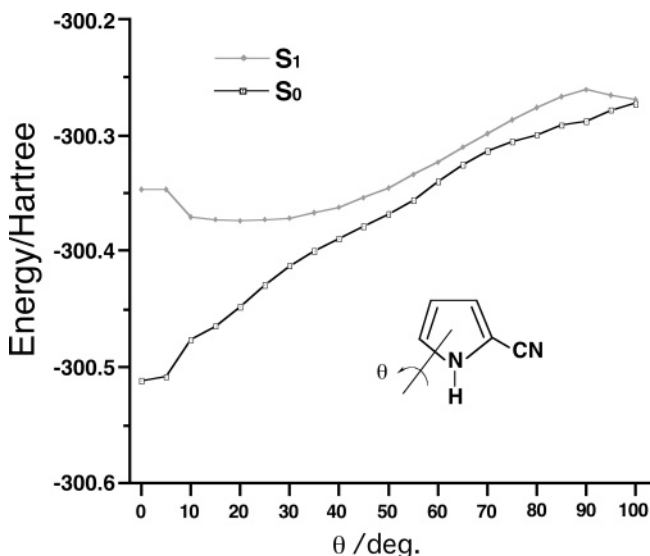
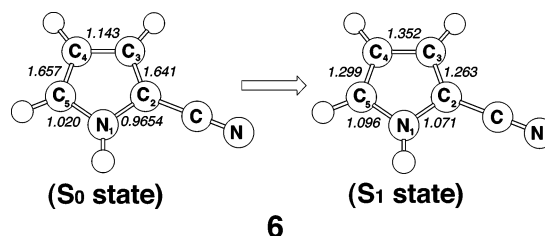


**Figure 1.** Minimum-energy pathway of 2-cyanopyrrole (**1**) along the torsion angle coordinate optimized for the  $S_1$  state at the CAS(8,7)/6-311G(d,p) level of theory.

lowers the energy of the excited state. Besides this, the formation of a degenerate point as a result of the rotation of the  $N$ – $C$  chemical bond strongly implies that a sloped  $S_0/S_1$  surface crossing<sup>14</sup> should exist at a very similar geometry. From there, decay to the ground state can be fully efficient.<sup>6</sup> Moreover, it should be mentioned that the return to  $S_0$  through a conical intersection at such a distorted quasi-tetrahedral geometry<sup>6</sup> is basically similar to both the  $H_4$ <sup>15a</sup> and the pericyclic<sup>15b,c</sup> models proposed previously.

Before proceeding further, one may wonder why rotation about the  $N_1$ – $C_5$  bond in the 2-cyanopyrrole (**1**) occurs more readily than in other chemical bonds in the five-membered ring. Basically, it is well-known that absorption of light leads to cleavage of the weakest of the chemical bonds in the ring.<sup>1</sup> According to the bond order analysis based on the CAS(8,7)/6-311G(d,p) level of theory, see **6**, it was found that the  $N_1$ – $C_2$  bond has the smallest bond order (1.071) in the  $S_1$  excited state of 2-cyanopyrrole (**1**). Accordingly, the theoretical finding strongly suggests that the  $N_1$ – $C_2$  bond should be the most facile to break in the excited 2-cyanopyrrole ring, which, in turn, can facilitate the rotation about the  $N_1$ – $C_5$  axis. We shall see the computational results supporting this prediction in the following section.



## IV. Results and Discussion

**2-Cyanopyrrole (1).** Let us first consider the photoisomerization of 2-cyanopyrrole (**1**). Two minimum-energy pathways on the singlet excited potential energy surface of **1** were characterized by optimizing the geometries along the  $C_2$ – $C_5$  coordinate (path I) and the  $N_1$ – $C_5$  coordinate (path II), which can lead to the same product (3-cyanopyrrole, **5**). For an understanding of the difference found between the two reaction paths, it is best to start the discussion with the reaction profiles as summarized in Figure 2, which also contains the relative energies of all the critical points with respect to the energy of the reactant **1**. Some selected geometrical parameters optimized for the stationary points and conical intersections are collected in Figure 3. The energies relative to the reactant molecule (**1**) are also listed in Table 1. Cartesian coordinates and energetics calculated for the various points at the CASSCF level are available as Supporting Information.

In the first step, the reactant (2-cyanopyrrole, **1**) is promoted to its excited singlet state by a vertical excitation as shown in the middle of Figure 2. After the vertical excitation process, the molecule is situated on the excited singlet surface but still possesses the  $S_0$  (ground-state) geometry (FC-A).<sup>12</sup> From the point reached by the vertical excitation the molecule relaxes to reach an  $S_1/S_0$  CI where the photoexcited system decays nonradiatively to  $S_0$ . Specifically, the photochemically active relaxation path, starting from the  $S_1$  ( $^1\pi_3 \rightarrow \pi_4^*$ ) excited state of 2-cyanopyrrole, leads to either  $S_1/S_0$  CI-1 (path I) or CI-2 (path II). These paths are shown in the left- and right-hand side of Figure 2, respectively.

The geometry at the conical intersection  $S_1/S_0$  CI-1 of  $C_1$  symmetry is shown in Figure 3. Our theoretical findings suggest

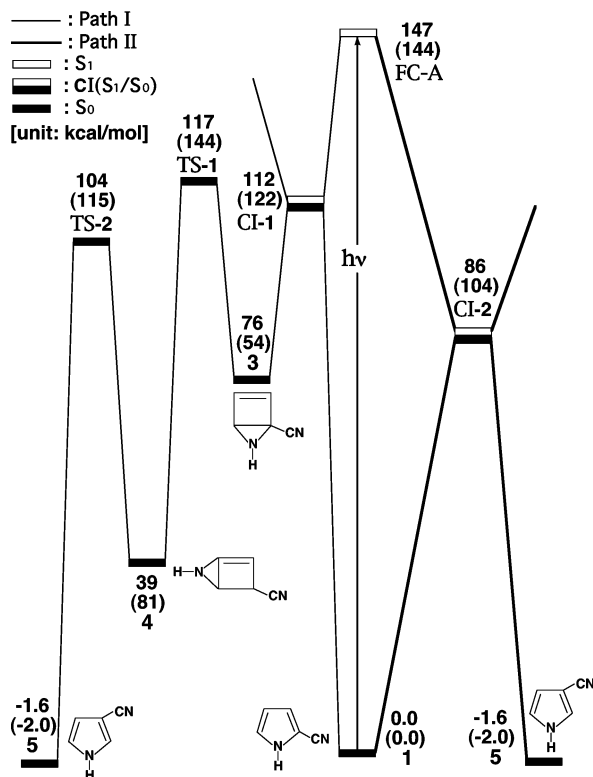


**Figure 2.** Energy profiles for the photoisomerization modes of 2-cyanopyrrole (**1**). The abbreviations FC and CI stand for Franck–Condon and conical intersection, respectively. The relative energies were obtained at the MP2–CAS–(8,7)/6-311G(d,p)//CAS(8,7)/6-311G(d,p) and CAS(8,7)/6-311G(d,p) (in parentheses) levels of theory. All energies (in kcal/mol) are given with respect to the reactant (**1**). The CASSCF optimized structures of the crucial points see Figure 3. For more information, see the text.

that  $S_1/S_0$  CI-1 is 112 kcal/mol lower in energy than FC-A at the MP2–CAS level of theory. The main difference between **1** and  $S_1/S_0$  CI-1 is found, apart from the nonplanar conformation, in the  $C_2$ – $C_5$  distance (2.018 Å), which is shorter, and the angle  $C_2N_1C_5$  (89.37°), which is considerably smaller in the latter. In Figure 3, we also give the directions of the derivative coupling and gradient difference vectors for the  $S_1/S_0$  CI-1 conical intersection. As a result, funneling through the  $S_1/S_0$  CI-1 conical intersection can lead to two different reaction pathways on the ground-state surface via either the derivative coupling vector or the gradient difference vector direction.<sup>6</sup> Any linear combination of these vectors causes the degeneracy to be lifted, and therefore these vectors give an indication of possible reaction pathways available on the ground-state surface after decay. As demonstrated in Figure 3, the major contribution of the derivative coupling vector involves the cyanopyrrole ring expanding, whereas the gradient difference vector corresponds to the concerted NCC out-of-plane bending motion. That is to say that the former becomes vibrationally hot at the **1**– $S_0$  configuration, whereas the latter allows the formation of bicyclic isomer **3** on the  $S_0$  potential energy surface. This intermediate is nonplanar, the nitrogen atom  $N_1$  being bent out of the ring plane. Then, a [1,3] sigmatropic shift of the NH group must take place<sup>16</sup> via a transition state (TS-1) to give another transient intermediate **4**. Again, this molecule has a nonplanar conformation. This then undergoes a ring opening via a transition state (TS-2) to form the final product 3-cyanopyrrole (**5**). That is to say that the computational results suggest that the mechanism for path I should proceed as follows: **1** → FC-A →  $S_1/S_0$  CI-1 → **3** → TS-1 → **4** → TS-2 → **5**. Besides these, our MP2–CAS

results indicate that the relative energetics of these critical points are 147, 112, 76, 117, 39, 104, and –1.6 kcal/mol for FC-A,  $S_1/S_0$  CI-1, **3**, TS-1, **4**, TS-2, and **5**, respectively, with respect to **1**. It is worth noting that FC-A lies 35 kcal/mol above  $S_1/S_0$  CI-1, whereas  $S_1/S_0$  CI-1 is only 5.0 kcal/mol below TS-1. Moreover, these **1** and **5** isomers are predicted to be nearly thermoneutral, with an exothermicity of less than 2 kcal/mol. Accordingly, our theoretical investigations suggest that the photoisomerization of **1** could adopt path I, as the species will have much excess energy and no means to dissipate it as the reactions are carried out in the gas phase and occur much faster than collisions.

Alternatively, as already shown in Figure 1, since the formation of a narrow energy gap between the  $S_1$  and  $S_0$  states found by twisting about one  $N_1$ – $C_5$  chemical bond strongly implies the existence of a conical intersection in a nearby geometry, geometry optimization on the  $S_1$  ( $\pi_3 \rightarrow \pi_4^*$ ) excited state is thus performed by rotating the  $N_1$ – $C_5$  bond. Thus, the lowest energy point of the intersection seam of the  $S_0$  and  $S_1$  states was located for reaction path II, which was identified as  $S_1/S_0$  CI-2 presented in Figures 2 and 3. Also, the orientation of the two vectors (i.e., the derivative coupling and gradient difference vectors) is given schematically in Figure 3. The derivative coupling vector for CI-2 corresponds to an antisymmetric stretching motion, which may lead to a vibrationally hot species at the  $S_0$  configuration. On the other hand, its gradient difference vector corresponds to the intramolecular rotation of a  $N_1$ – $C_2$  bond. Indeed, the most characteristic feature in the geometry of  $S_1/S_0$  CI-2 is that one  $N_1$ – $C_5$  ring bond lies out of the molecular plane as predicted in the previous section. Namely, in forming such a conical intersection structure, planarity is lost and one  $N_1$ – $C_5$  ring bond moves out of plane by about 84°. Therefore, from the structure at the  $S_1/S_0$  CI-2 point, the nature of the relaxation path II on the  $S_1$  potential surface can be regarded as  $N_1$ – $C_2$  bond cleavage leading to the exchange of two neighboring atoms. These calculations thus reveal that the geometry of the conical intersection, from which it undergoes intramolecular rotation, is approaching the planar geometry of 3-cyanopyrrole (**5**). Furthermore, as shown in Figure 2, the geometry optimization starting from FC-A leads to  $S_1/S_0$  CI-2, the latter being approximately 61 kcal/mol lower in energy than the former. In particular, it is noted that  $S_1/S_0$  CI-2 is energetically more favored than  $S_1/S_0$  CI-1 by 26 kcal/mol. This strongly indicates that path II is more favorable than path I.

On the basis of the above discussion, we propose a picture of the photochemistry of **1**, which is already schematically shown in Figure 2. Comparing the two reaction pathways (path I and path II), our ab initio CASSCF and MP2–CAS calculations show that path II is preferred over path I. That is, an efficient photoisomerization occurs when the photoexcited reactant FC-A evolves along a barrierless excited-state pathway, decays at a conical intersection point ( $S_1/S_0$  CI-2) and finally relaxes to the ground state between reactant (**1**) and photoproduct (**5**).

**2-Cyano-5-Methylpyrrole (2).** Like the case of 2-cyanopyrrole (**1**), the photoisomerization reactions of 2-cyano-5-methylpyrrole (**2**) studied in this work follow similar reaction paths to those shown earlier. That is, the reaction profiles computed for eq 4 of the model compound **2** (Figure 4) resemble that of **1**. Figure 4 is thus arranged as Figure 2, its center indicating the reactant **2** ( $S_0$ ) and FC-B ( $S_0$  geometry). Also, the reaction profiles, obtained by optimizing the geometries along the courses of isomerization paths, are depicted to the left- (path III and

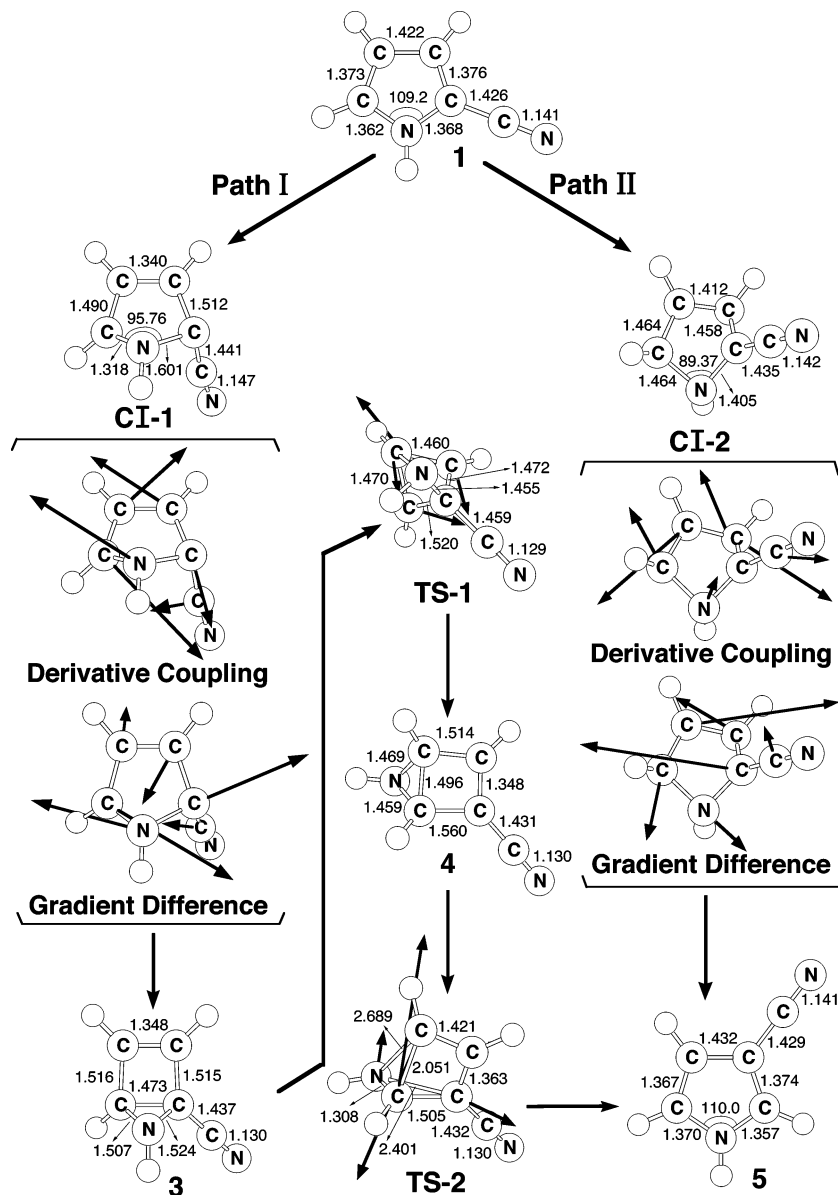


**Figure 3.** The CAS(8,7)/6-311G(d,p) geometries (in Å and deg) for 2-cyanopyrrole (**1**), conical intersection (CI), intermediate, transition state (TS), and isomer products. The derivative coupling and gradient difference vectors—those that lift the degeneracy—computed with CASSCF at the conical intersections CI-1 and CI-2. (Inset) Corresponding CASSCF vectors. For more information, see the Supporting Information.

**TABLE 1: Energies (in kcal/mol) of the Critical Points Located along the Pathways I and II at the MP2-CAS-(8,7)/6-311G(d,p)//CAS(8,7)/6-311G(d,p) and CAS(8,7)/6-311G(d,p) (in parentheses) Levels of Theory<sup>a</sup>**

structure	state	$\Delta E_{\text{rel}}^b$
2-cyanopyrrole ( <b>1</b> )	$S_0$	0.0 (0.0)
FC-A	$S_1$	147.1 (143.6)
CI-1	$S_1/S_0$	111.6 (122.1)
<b>3</b>	$S_0$	75.94 (53.73)
TS-1	$S_0$	117.2 (143.5)
<b>4</b>	$S_0$	39.31 (80.53)
TS-2	$S_0$	103.8 (114.9)
CI-2	$S_1/S_0$	86.33 (104.2)
3-cyanopyrrole ( <b>5</b> )	$S_0$	-1.602 (-1.953)

<sup>a</sup> See Figures 2 and 3. <sup>b</sup> Energy relative to 2-cyanopyrrole.

IV) and the right-hand (path V) side, respectively. The energies relative to the reactant molecule (**2**) are summarized in Table 2. Selected optimized geometrical parameters for the various points can be taken from Figure 5. Cartesian coordinates and energetics calculated for the various points at the CASSCF level are available as Supporting Information.

The vertical excitation energy (FC-B;  ${}^1(\pi_3 \rightarrow \pi_4^*)$ ) is calculated to lie 161 kcal/mol above the ground-state surface at the CAS(8,7)/6-311G(d,p) optimized reactant geometry **2**. This value drops to 148 kcal/mol after correction using MP2-CAS calculations, which is nearly equivalent to that of 2-cyanopyrrole **1** (147 kcal/mol). As there are no relevant experimental and theoretical data on such a molecule, the above result is a prediction.

From the point reached by the vertical excitation FC-B, the molecule can return to the ground state via two radiationless decay routes (paths III and IV). The first step of both involves a conical intersection  $S_1/S_0$  CI-3, and leads eventually to the production of 3-cyano-2-methylpyrrole (**8**) and 3-cyano-4-methylpyrrole (**10**), respectively. The geometrical structure of  $S_1/S_0$  CI-3 can be found in Figure 5, which also contains the derivative coupling and gradient difference vectors. The geometry of this conical intersection is quite similar to the geometry found for  $S_1/S_0$  CI-1 of the 2-cyanopyrrole (**1**) system. The derivative coupling vector in CI-3 corresponds to the antisymmetric bending motion of the five-membered ring, which can

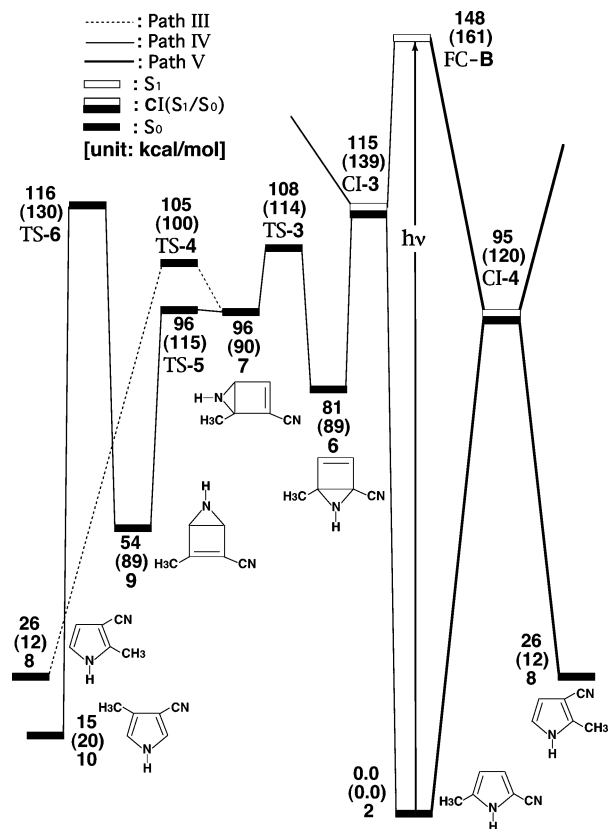


**Figure 4.** Energy profiles for the photoisomerization modes of 2-cyano-5-methylpyrrole (**2**). The abbreviations FC and CI stand for Franck–Condon and conical intersection, respectively. The relative energies were obtained at the MP2–CAS–(8,7)/6-311G(d,p)//CAS(8,7)/6-311G–(d,p) and CAS(8,7)/6-311G(d,p) (in parentheses) levels of theory. All energies (in kcal/mol) are given with respect to the reactant (**2**). The CASSCF optimized structures of the crucial points, see Figure 5. For more information, see the text.

**TABLE 2: Energies (in kcal/mol) of the Critical Points Located along the Pathways III, IV, and V at the MP2–CAS–(8,7)/6-311G(d,p)//CAS(8,7)/6-311G(d,p) and CAS(8,7)/6-311G(d,p) (in parentheses) Levels of Theory<sup>a</sup>**

structure	state	$\Delta E_{\text{rel}}^b$
2-cyano-5-methylpyrrole ( <b>2</b> )	S <sub>0</sub>	0.0 (0.0)
FC–B	S <sub>1</sub>	148.1 (160.7)
CI-3	S <sub>1</sub> /S <sub>0</sub>	115.2 (138.6)
<b>6</b>	S <sub>0</sub>	81.07 (88.55)
TS-3	S <sub>0</sub>	107.9 (114.4)
<b>7</b>	S <sub>0</sub>	95.54 (90.19)
TS-4	S <sub>0</sub>	105.2 (100.2)
3-cyano-2-methylpyrrole ( <b>8</b> )	S <sub>0</sub>	26.42 (11.51)
TS-5	S <sub>0</sub>	96.25 (114.8)
<b>9</b>	S <sub>0</sub>	53.83 (89.40)
TS-6	S <sub>0</sub>	115.5 (129.7)
3-cyano-4-methylpyrrole ( <b>10</b> )	S <sub>0</sub>	14.55 (19.80)
CI-4	S <sub>1</sub> /S <sub>0</sub>	94.63 (120.2)

<sup>a</sup> See Figures 4, 5, and 6. <sup>b</sup> Energy relative to 2-cyano-5-methylpyrrole.

lead to a vibrationally hot 2–S<sub>0</sub> configuration. Following the gradient difference vector from S<sub>1</sub>/S<sub>0</sub> CI-3 and decreasing the C<sub>2</sub>–C<sub>5</sub> distance, as seen in Figures 4 and 5, leads to either the formation of the bicyclic intermediate **6** or a back reaction to the reactant **2**. Then, the system undergoes a 1,3-sigmatropic shift of the NH group via a transition state TS-3 to give another bicyclic species **7**. From there the isomerization can take place in two directions: the ring opening to produce 3-cyano-2-methylpyrrole (**8**) product (path III), or the NH group transfer

to the other C–C ring bond leading to the formation of 3-cyano-4-methylpyrrole (**10**) product (path IV). As a result, our theoretical investigations suggest that the reaction mechanisms for path III and path IV should proceed as follows: **2** → FC–B → S<sub>1</sub>/S<sub>0</sub> CI-3 → **6** → TS-3 → **7** → TS-4 → **8** and **2** → FC–B → S<sub>1</sub>/S<sub>0</sub> CI-3 → **6** → TS-3 → **7** → TS-5 → **9** → TS-6 → **10**. From Figure 4, it is apparent that the transition state TS-6 for intermediate **9** to product **10** is the only transition state (116 kcal/mol) that lies slightly above the energy of S<sub>1</sub>/S<sub>0</sub> CI-3 (115 kcal/mol). This strongly implies that the bicyclic intermediate (**7**) is kinetically unstable and may rearrange spontaneously to the more stable minima (**8**) if it is produced. This, in turn, would lead to the path III photoproduct (**8**) in a larger yield than the path IV photoproduct (**10**). The supporting evidence comes from the fact that, as mentioned in eq 4, one major product (**8**) and one minor product (**10**) were observed in the photoisomerization reaction of 2-cyano-5-methylpyrrole (**2**).<sup>3,4</sup>

On the other hand, like the case of 2-cyanopyrrole **1**, we also explore the mechanism of path V, which only contains one conical intersection point (S<sub>1</sub>/S<sub>0</sub> CI-4). The derivative coupling and gradient difference vectors obtained at the conical intersection are also given in Figure 6. As seen in the right-hand side of Figure 4, the MP2–CAS results suggest that S<sub>1</sub>/S<sub>0</sub> CI-4 is lower than FC–B by 53 kcal/mol in energy, while the competing S<sub>1</sub>/S<sub>0</sub> CI-3 is higher than S<sub>1</sub>/S<sub>0</sub> CI-4 by 20 kcal/mol in energy. The existence of a low-lying conical intersection provides a highly effective radiationless decay channel.<sup>6</sup> Accordingly, our model calculations indicate that path V is more favorable than path III (and path IV) from both energetic and practical viewpoints. Also, the computations predict that the photochemical rearrangement reaction of path V should be a barrierless process. That is, starting from the FC–B point, 2-cyano-5-methylpyrrole (**2**) enters an extremely efficient decay channel, S<sub>1</sub>/S<sub>0</sub> CI-4. After decay at this conical intersection point, the photoisomer **8** as well as the initial reactant **2** can be reached via a barrierless ground-state relaxation pathway.

In short, our model investigations demonstrate that upon absorption of a photon of light, 2-cyano-5-methylpyrrole (**2**) is excited vertically to S<sub>1</sub> (FC–B). From this point, the system can return to the ground state via three radiationless decay routes (path III, path IV, and path V). In particular, path III and path V are competing with each other, the former being energetically feasible from a kinetic viewpoint. Moreover, for path V, **2** in the S<sub>1</sub> state proceeds to rotate one N=C bond via a conical intersection and, subsequently, returns to the ground state nonradiatively to give 3-cyano-2-methylpyrrole (**8**) without any intermediates. This results in **8** as the only major product. The present calculations also indicate that the energy of the transition state (TS-6) for path IV is somewhat greater than that of the corresponding conical intersection (S<sub>1</sub>/S<sub>0</sub> CI-3). This suggests that path IV should be of less important than path III, and that 3-cyano-4-methylpyrrole (**10**) should be the minor product. All these theoretical findings are in accordance with the experimental observations.<sup>3,4</sup>

## V. Extensions

In fact, the photochemical formation of unstable isomers leading to a shift of ring atoms seems to be a general process in the photochemistry of heterocyclic compounds.<sup>1</sup> The molecules that we have studied in the previous sections all have planar ring geometries with one electronegative atom. Nevertheless, the analysis of photochemical rearrangements can easily be extended to other cyclic molecules with several heteroatoms.

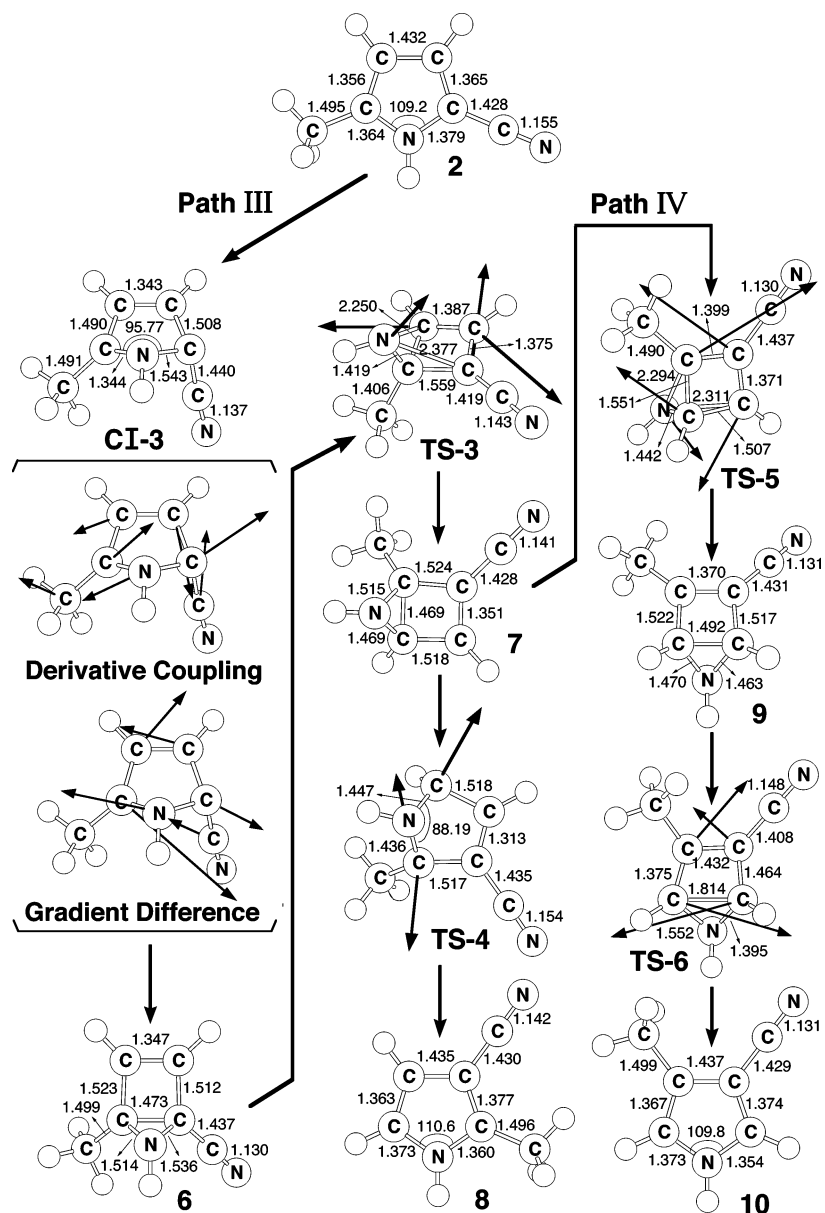


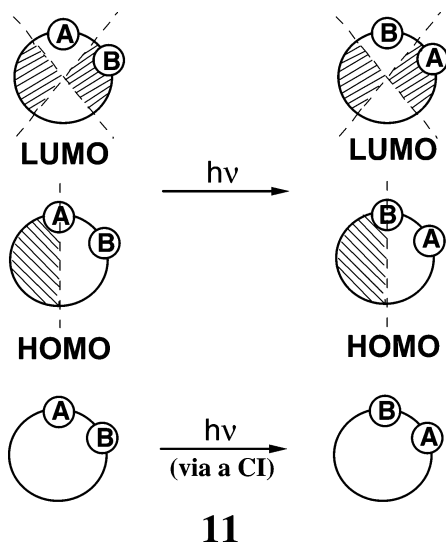
**Figure 5.** The CAS(8,7)/6-311G(d,p) geometries (in Å and deg) for path III and path IV of 2-cyano-5-methylpyrrole (2), conical intersection (CI), intermediate, transition state (TS), and isomer products. The derivative coupling and gradient difference vectors—those that lift the degeneracy—computed with CASSCF at the conical intersections CI-3. (Inset) Corresponding CASSCF vectors. For more information, see the Supporting Information.

If such heterocyclic molecules absorb a photon to go to an excited singlet state, and the nature of its photoexcitation is consistent with a  ${}^1(\pi_{\text{HOMO}} \rightarrow \pi^*_{\text{LUMO}})$  transition, then the central novel results for the photochemistry of heterocyclics are the existence of conical intersections. That is, when a heterocyclic molecule absorbs a photon to go to an excited state, then the system enters an extremely efficient decay channel, which takes the form of a conical intersection between the excited- and ground-state potential energy surfaces.<sup>6</sup> After decay at the conical intersection, the system continues its evolution on the ground state to produce new chemical species.

Besides, geometries at which conical intersections are likely to occur may be predicted by means of simple models. Let us take the present heterocyclic systems as an example to demonstrate the prediction of conical intersection geometry. Suppose that the heterocyclic molecule bears at least one electronegative atom. The  $p$ - $\pi$  frontier orbital structure of the heterocyclic ring can be described in terms of nodal planes as shown in **11**.<sup>17</sup>

Basically, the HOMO of the heterocyclic molecule is an occupied antibonding  $\pi$  orbital with the most electronegative heteroatom (e.g., A) lying along the nodal plane. Additionally, the LUMO of the reactant usually bears two nodal planes, which bisect A and B heteroatoms as illustrated schematically in **11**. From the two-electron and two-orbital (HOMO and LUMO) model for heterocyclics, it follows that certain perturbations that induce a splitting of the  $p$ - $\pi$  orbitals in the heterocyclic compound will lower the energy separation between the ground (e.g.,  $S_0$ ) and excited (e.g.,  $S_1$ ) states. Once the perturbation reaches a value, which reduces the energy separation to zero, it results in a conical intersection.<sup>6</sup> Thus, as already demonstrated in this study, rotating a heterocyclic ring bond can greatly decrease the energy gap between the HOMO and LUMO, and eventually a conical intersection is reached. As a result, for heterocyclic molecules, it is the topology of the  $p$ - $\pi$  orbitals shown in **11** that can generate the interchange of A and B atoms via conical intersections. A more detailed account of the

photochemical mechanisms of various heterocyclic reactions obtained from calculations using the topological model (11) will be given elsewhere.<sup>18</sup>



## VI. Conclusion

We have studied the reaction mechanisms of photoreactions of 2-cyanopyrrole (eq 1) and 2-cyano-5-methylpyrrole (eq 4), with respect to permutation of the ring atoms. Taking all these systems studied in this paper together, one can draw the following conclusions:

(1) From the present results, we can elaborate on the standard model of the photochemistry of cyanopyrrole and of its methyl substituted derivatives. It is found that knowledge of the conical intersection of the pyrrole species is of great importance in understanding its reaction mechanism since it can affect the driving force for photochemistry. For instance, cyanopyrrole is vertically excited to the  $S_1$  state. Then, radiationless decay from  $S_1$  to  $S_0$  of cyanopyrrole occurs via a conical intersection, which results in a rapid ring bond rotation. Starting from this conical intersection, the products of the phototranspositions as well as the initial reactant can be reached on a barrier-less ground-state relaxation path. As a result, these findings, based on the conical intersection viewpoint, have helped us to better understand the photochemical reactions, and to support the experimental observations.<sup>2-4</sup>

(2) It has been generally assumed in the past that the photoisomerization of cyanopyrroles follows the internal cyclization-isomerization sequence.<sup>1,4,5</sup> This mechanism involves an initial disrotatory formation of a bicyclic isomer, followed by a [1,3] sigmatropic shift to a second bicyclic isomer. This then undergoes a disrotatory ring opening to yield the rearranged product. However, our model investigations indicate that this mechanism involves several high energy transition structures, which makes it energetically unfeasible from a kinetic viewpoint.

(3) In this work, we propose a simple  $p$ - $\pi$  orbital topology model, which can be used as a guide to predict the location at which conical intersections are likely to occur, as well as the conformations of the phototransposition products of various heterocycles. The results presented here, together with our work on the photochemistry of other 5- and six-membered heterocycles,<sup>18</sup> appear to give convincing evidence that conical intersections play a key role in such photoisomerizations, and that they are directly involved in heterocycle photochemistry and photophysics.

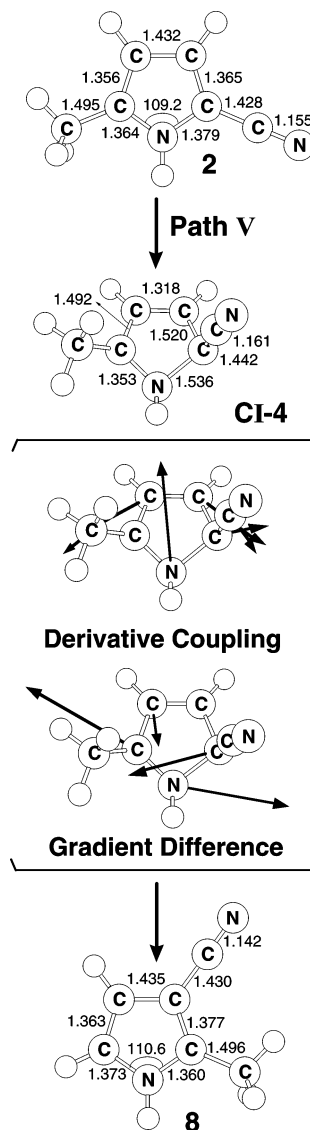


**Figure 6.** The CAS(8,7)/6-311G(d,p) geometries (in Å and deg) for path V of 2-cyano-5-methylpyrrole (2), conical intersection (CI), and isomer product. The derivative coupling and gradient difference vectors—those that lift the degeneracy—computed with CASSCF at the conical intersections CI-4. (Inset) Corresponding CASSCF vectors. For more information, see the Supporting Information.

It is hoped that the present work can stimulate further research into this subject.

**Acknowledgment.** I am grateful to the National Center for High-Performance Computing of Taiwan for generous amounts of computing time and the National Science Council of Taiwan for the financial support. I also wish to thank Professor Michael A. Robb, Dr. Michael J. Bearpark, (University of London, UK), Professor Massimo Olivucci (Universita degli Studi di Siena, Italy), and Professor Fernando Bernardi (University of Bologna, Italy) for their encouragement and support during my stay in London. Special thanks are also due to Referee 66 and Referee 69 for very helpful suggestions and comments.

**Supporting Information Available:** Details for the optimized atomic coordinates and energies of compounds studied in this work are available in PDF format. This material is available free of charge via the Internet at <http://pubs.acs.org>.



## References and Notes

- (1) For reviews, see: (a) De Mayo, P. In *Rearrangements in Ground and Excited States*; Academic Press: New York, 1980; Vol. 3, p 501. (b) Buchardt, O. In *Photochemistry of Heterocyclic Compounds*; Wiley: New York, 1976. (c) Kopecky, J. In *Organic Photochemistry: A Visual Approach*; VCH Publishers: New York, 1992.
- (2) Hiraoka, H. *Chem. Commun.* **1970**, 1306.
- (3) Barltrop, J.; Day, A. C.; Moxon, P. D.; Ward, R. W. *Chem. Commun.* **1975**, 786.
- (4) Barltrop, J.; Day, A. C.; Ward, R. W. *Chem. Commun.* **1978**, 131.
- (5) Behrens, S.; Jug, K. *J. Org. Chem.* **1990**, 55, 2288.
- (6) (a) Bernardi, F.; Olivucci, M.; Robb, M. A. *Isr. J. Chem.* **1993**, 265. (b) Klessinger, M. *Angew. Chem., Int. Ed. Engl.* **1995**, 34, 549. (c) Bernardi, F.; Olivucci, M.; Robb, M. A. *Chem. Soc. Rev.* **1996**, 321. (d) Bernardi, F.; Olivucci, M.; Robb, M. A. *J. Photochem. Photobiol. A: Chem.* **1997**, 105, 365. (e) Klessinger, M. *Pure Appl. Chem.* **1997**, 69, 773.
- (7) Frisch, M. J.; Trucks, G. W.; Schlegel, H. B.; Scuseria, G. E.; Robb, M. A.; Cheeseman, J. R.; Montgomery, J. A., Jr.; Vreven, T.; Kudin, K. N.; Burant, J. C.; Millam, J. M.; Iyengar, S. S.; Tomasi, J.; Barone, V.; Mennucci, B.; Cossi, M.; Scalmani, G.; Rega, N.; Petersson, G. A.; Nakatsuji, H.; Hada, M.; Ehara, M.; Toyota, K.; Fukuda, R.; Hasegawa, J.; Ishida, M.; Nakajima, T.; Honda, Y.; Kitao, O.; Nakai, H.; Klene, M.; Li, X.; Knox, J. E.; Hratchian, H. P.; Cross, J. B.; Bakken, V.; Adamo, C.; Jaramillo, J.; Gomperts, R.; Stratmann, R. E.; Yazyev, O.; Austin, A. J.; Cammi, R.; Pomelli, C.; Ochterski, J. W.; Ayala, P. Y.; Morokuma, K.; Voth, G. A.; Salvador, P.; Dannenberg, J. J.; Zakrzewski, V. G.; Dapprich, S.; Daniels, A. D.; Strain, M. C.; Farkas, O.; Malick, D. K.; Rabuck, A. D.; Raghavachari, K.; Foresman, J. B.; Ortiz, J. V.; Cui, Q.; Baboul, A. G.; Clifford, S.; Cioslowski, J.; Stefanov, B. B.; Liu, G.; Liashenko, A.; Piskorz, P.; Komaromi, I.; Martin, R. L.; Fox, D. J.; Keith, T.; Al-Laham, M. A.; Peng, C. Y.; Nanayakkara, A.; Challacombe, M.; Gill, P. M. W.; Johnson, B.; Chen, W.; Wong, M. W.; Gonzalez, C.; Pople, J. A. *Gaussian 03*, revision x.xx; Gaussian, Inc.: Pittsburgh, PA, 2003.
- (8) Bearpark, M. J.; Robb, M. A.; Schlegel, H. B. *Chem. Phys. Lett.* **1994**, 223, 269.
- (9) McDouall, J. J. W.; Peasley, K.; Robb, M. A. *Chem. Phys. Lett.* **1988**, 148, 183.
- (10) Jorgensen, W. J.; Salem L. In *The Organic Chemist's Book of Orbitals*; Academic Press: New York, 1973; pp 231.
- (11) Anderson, H. J. *Can. J. Chem.* **1959**, 37, 2053.
- (12) (a) The  $S_1$  excited state created by direct excitation of a cyanopyrrole is a vertical state with the same geometry as the ground state ( $S_0$ ) molecule. (b) An excited state with geometry identical to the ground state is called a Franck-Condon (FC) state.
- (13) The C-C, C-N, C-H, and N-H bonds in 2-cyanopyrrole (**1**) are fixed to be 1.35, 1.35, 1.09, and 1.09 Å, respectively. Also, the  $\angle CCC$ ,  $\angle CNC$ ,  $\angle HCC$ ,  $\angle HNC$ , and  $\angle CCN$  bond angles are fixed to be 108, 108, 126, 126, and 180°, respectively.
- (14) Xantheas, S. S.; Rudenberg, K. *J. Chem. Phys.* **1991**, 95, 1862.
- (15) (a) Gerhartz, W.; Poshusta, R. D.; Michl, J. *J. Am. Chem. Soc.* **1977**, 99, 4263. (b) Olivucci, M.; Ragazos, I. N.; Bernardi, F.; Robb, M. A. *J. Am. Chem. Soc.* **1993**, 115, 3710. (c) Olivucci, M.; Bernardi, F.; Celani, P.; Ragazos, I. N.; Robb, M. A. *J. Am. Chem. Soc.* 1994, 116, 1077.
- (16) In contrast to a [1,3] sigmatropic hydrogen migration, the migration of the NH group is Woodward-Hoffmann allowed since a p orbital at nitrogen is participating in the reaction which allows a change of sign of the concerted molecular orbital.
- (17) Albright, T. A.; Burdett, J. K.; Whangbo, M. H. *Orbital Interaction in Chemistry*; Wiley: New York, 1985; pp 84.
- (18) Su, M.-D. *J. Phys. Chem. A* **2006**, 110, 9420.